

Average properties of bidisperse bubbly flowsJ. C. Serrano-García,¹ S. Mendez-Díaz,² and R. Zenit^{1,*}¹*Instituto de Investigaciones en Materiales, Universidad Nacional Autónoma de México, Apdo. Postal 70-360, México Distrito Federal 04510, México*²*Facultad de Ingeniería Mecánica y Eléctrica, Universidad Autónoma de Nuevo León, Pedro de Alba s/n, Ciudad Universitaria, San Nicolas de los Garza, 46451, Nuevo León, México*

(Received 25 October 2017; published 21 March 2018)

Experiments were performed in a vertical channel to study the properties of a bubbly flow composed of two distinct bubble size species. Bubbles were produced using a capillary bank with tubes with two distinct inner diameters; the flow through each capillary size was controlled such that the amount of large or small bubbles could be controlled. Using water and water-glycerin mixtures, a wide range of Reynolds and Weber number ranges were investigated. The gas volume fraction ranged between 0.5% and 6%. The measurements of the mean bubble velocity of each species and the liquid velocity variance were obtained and contrasted with the monodisperse flows with equivalent gas volume fractions. We found that the bidispersity can induce a reduction of the mean bubble velocity of the large species; for the small size species, the bubble velocity can be increased, decreased, or remain unaffected depending of the flow conditions. The liquid velocity variance of the bidisperse flows is, in general, bound by the values of the small and large monodisperse values; interestingly, in some cases, the liquid velocity fluctuations can be larger than either monodisperse case. A simple model for the liquid agitation for bidisperse flows is proposed, with good agreement with the experimental measurements.

DOI: [10.1103/PhysRevFluids.3.034306](https://doi.org/10.1103/PhysRevFluids.3.034306)**I. INTRODUCTION**

Bubbly flows, a two-phase gas-liquid flow in which the gas is discretely dispersed inside a liquid, are common in many natural phenomena as well as in many engineering applications. The case in which bubbles rise in a quiescent liquid is of particular importance and interest for understanding bubble reactors [1]. In particular, it is of practical interest to determine the level of liquid velocity fluctuations, often called pseudoturbulence [2–4]. Many recent studies have addressed this issue and much progress has been reached; the recent review paper by Risso [5] gives a comprehensive view of the state of the art of the subject. It has been found that for the bubble phase, the agitation is caused primarily by the wake-induced path instability. For the liquid phase, the agitation can be attributed to arise from either the anisotropic flow disturbances generated near the bubbles or the isotropic disturbance that results from the spatial population of bubbles in the liquid.

Despite the progress in the understanding of these flows, most fundamental arguments have been constructed from an idealized state: a monodisperse bubbly flow. So, we must ask: How applicable are these results to real flows in which the bubble size distribution is polydisperse? When the bubble size is not distributed closely around one dominant size, additional mechanisms of bubble-bubble interactions can be expected which could, perhaps, lead to a different collective behavior. This paper addresses this very issue.

*zenit@unam.mx

The simplest case of polydispersity is that in which the dispersed phase size is distributed around two distinct sizes: a bidisperse flow. Surprisingly, while other types of bidisperse two-phase flows have been analyzed, only a few studies of bidisperse bubbly flows have appeared in the published literature. In particular, to our knowledge, no previous experimental data of such flows exist.

Batchelor [6] and Batchelor and Wen [7] studied the sedimentation of dilute polydisperse system of solid spheres at small Reynolds numbers. They derived expressions for the mean sedimentation velocity for each size species, considering only pair interactions. They generalized the calculation proposed by Batchelor [8]. For the case of a bidisperse sedimenting suspension, considering only two-species of two distinct sizes, large and small (L and S), the mean sedimenting velocity of each size species can be written as

$$U^S = U_{\text{term}}^S (1 + S_{SS}\alpha^S + S_{SL}\alpha^L), \quad (1)$$

$$U^L = U_{\text{term}}^L (1 + S_{LL}\alpha^L + S_{LS}\alpha^S), \quad (2)$$

where α^S and α^L are the volume fractions of each species. The coefficients S_{SS}, S_{SL}, S_{LS} and S_{LL} are sedimentation coefficients. The terminal velocity U_{term}^i (for i being either L or S) depends on diameter, density difference and fluid viscosity. Peysson and Guazzelli [9] conducted experiments to measure S_{ij} in this regime. They found some agreement with the predictions, but important differences were also identified.

For this low Re regime, Weiland *et al.* [10] conducted experiments on bidisperse sedimenting suspensions. They discovered that, under certain conditions, particularly for relatively large concentrations, particles of each species gathered together and developed vertical streaming motion with much larger magnitudes than the sedimenting velocity of at least one of the two types of particles. Batchelor and Rensburg [11] confirmed this finding considering a wider range of parameters.

For the case of sedimenting suspension for which the particle Stokes number is large (solid particles in a gas), there have been several theoretical studies. Kumaran and Koch [12,13] obtained explicit formulas for the sedimenting velocity of particles and velocity fluctuations. Valiveti and Koch [14] calculated the stability of such flows and found limits of homogenous sedimentation. Abbas *et al.* [15] investigated both sedimentation and shear flows of bidisperse suspensions with numerical simulations for small Reynolds and Stokes numbers. They found that for size ratios up to 2.5 the concentration fluctuation levels could be strongly enhanced.

The case of bidisperse bubbly flows has received much less attention. Kumaran and Koch [16] studied the effect of hydrodynamic interactions on the average properties of a bidisperse suspension of high Reynolds number, low Weber number bubbles. They considered pair-wise interactions in potential flow. By considering different size ratios, they calculated the terminal velocity of each bubble species. For size ratios close to 1, the interaction was found to slow down the large bubble velocity. When the size ratio as decreased, the opposite effect was observed. This study was the first to address the effect of interactions of different bubble sizes in the mean bubble velocity. As explained below, these findings are in good qualitative agreement with the present results.

Goz *et al.* [17] first showed that bidisperse bubbly flows could be studied by numerical means. They argued that parameters like bubble size, deformability, void fraction, and polydispersity could be varied to analyze bubble interaction, swarm velocity, and bubble-induced liquid turbulence. Subsequently, Goz and Sommerfeld [18] conducted additional simulations and found that the small bubble species would be significantly affected by large ones: they observed small bubbles entering the wake of the larger bubbles. These studies, however, served only as a proof-of-concept and no further in depth analysis of the dynamics of the such flows were reported. In the study by Lu and Tryggvason [19], some bidisperse simulation results were reported. They found that the difference between flows with bubbles of two sizes and flows with only one size were relatively small, as long as the size difference was not too large and the void fraction was the same. More recently, Roghair *et al.* [20] and Santarelli and Frohlich [21] also conducted numerical simulations of bubbly flows. Both studies found that bidisperse flow behaved similarly to monodisperse flows. Santarelli and Frohlich

TABLE I. Physical properties of the test liquids: water and water-glycerin (w-g) mixtures. Morton number: $Mo = g\mu^4/\rho\sigma^3$.

Liquid (symbol)	ρ kg/m ³	σ N/m ²	μ Pa s	Mo (-)
water (●) or (○)	998.20	72.04×10^{-3}	1.00×10^{-3}	2.63×10^{-8}
w-g 30% (◆) or (◇)	1079.30	66.56×10^{-3}	3.35×10^{-3}	3.88×10^{-6}
w-g 50% (□) or (■)	1126.30	64.57×10^{-3}	5.58×10^{-3}	3.134×10^{-5}

[21] reported that the fluctuation levels of the small bubbles in the bidisperse swarm were higher than the corresponding monodisperse case, in agreement with the results of Goz *et al.* [17]. To our knowledge, no previous experimental studies of bidisperse bubbly flows have been published.

In this paper, experimental measurements of the bubble velocity and liquid velocity variance are presented for a range of gas volume fractions and for different liquids to cover a wide range of Reynolds and Weber numbers. The effect of bidispersity is characterized by the ratio of gas volume fractions, R .

II. EXPERIMENTAL SETUP AND MEASUREMENT TECHNIQUES

The experimental setup is similar to that used by Martinez-Mercado *et al.* [2] and Mendez *et al.* [4]. It consists of a vertical acrylic column with a rectangular cross-section of 12×5 cm². At the bottom of the column, a bank of capillaries is connected through flanges. The column was filled with different liquids: water and water-glycerin mixtures. The physical properties of the liquids used here are listed in Table I. To reduce the amount of coalescence, a small amount of salt (MgSO₄, by Aldrich 63138, 99.5% purity) was added to all the liquids [2].

The mean gas volume fraction, α , was measured from the column hold up. The following expression was used:

$$\alpha = \left(1 + \frac{H_o}{\Delta H}\right)^{-1}, \quad (3)$$

where H_o is the height of liquid without bubbles and ΔH is the increase in height that results after the bubbles have been introduced in the column. For this study, seven values of the gas volume fraction were considered: $\alpha = [0.005, 0.01, 0.02, 0.03, 0.04, 0.05, 0.06]$. The same seven conditions were tested for all cases. For all the results shown here, $H_o = 1.0$ m and was kept fixed for all the experiments. The flows did not show a significant inhomogeneous bubble distribution within the width of the channel. Since the conditions were similar to those of Zenit *et al.* [22], no further measurements of the homogeneity were conducted.

The bank of capillaries, which is the most important part of this experimental array, was designed to generate a bidisperse bubbly flow based on the ideas of Zenit *et al.* [22] and Martinez-Mercado *et al.* [2] to produce a monodisperse bubbly flow. To generate two different bubble sizes, the bank had capillaries of two different internal diameters; each capillary type was connected to a different gas chamber. Using needle valves, the flow rate of Nitrogen through each chamber was controlled. In this manner, it was possible to generate bidisperse bubbly flows in which the amount of bubbles of each size was controlled. Figure 1 shows a schematic representation of the dual-chamber arrangement. The internal diameters of the two capillary tubes were 0.20 and 1.19 mm to generate small and large bubbles, respectively. With these tubes, bubble diameters of 1.7 and 3.7 mm (for the case of individual bubbles in water) were produced.

In this investigation we considered the combined effect of two bubble sizes in the average properties on the flow. The superscript “L” or “S” will be used throughout the paper to refer to

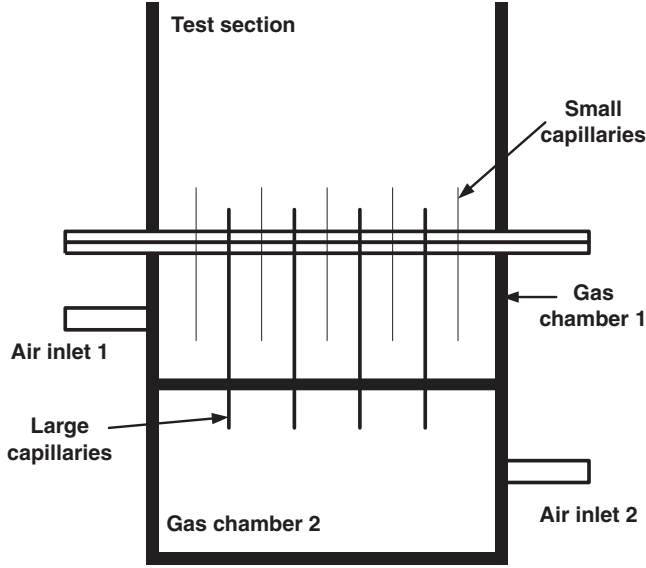


FIG. 1. Scheme of the capillary array.

large or small bubbles, respectively. Therefore, the bubble size ratio is defined as

$$\lambda = \frac{d_{\text{eq}}^L}{d_{\text{eq}}^S}, \quad (4)$$

where d_{eq} is the equivalent bubble diameter calculated as $d_{\text{eq}} = \sqrt[3]{d_{\text{large}}^2 d_{\text{short}}}$, where d_{large} and d_{short} are the large and short side of the 2D photographic image of a given ellipsoidal bubble. Also, the bubble aspect ratio is defined as $\chi = d_{\text{large}}/d_{\text{short}}$.

The bubble velocity ratio is defined as

$$\Gamma_1 = \frac{U_b^L}{U_b^S}, \quad (5)$$

where U_b^i is the mean bubble velocity of the i th species. The ratio of liquid velocity variances is

$$\Gamma_2 = \frac{\langle U_l^2 \rangle^L}{\langle U_l^2 \rangle^S}, \quad (6)$$

where $\langle U_l^2 \rangle^L$ and $\langle U_l^2 \rangle^S$ is the variance of the liquid velocity for large and small bubbles, respectively.

Last, the gas volume fraction ratio is defined as

$$R = \frac{\alpha^L}{\alpha^S}, \quad (7)$$

where α^i is the gas volume fraction of each bubble species. The total gas volume fraction is given by $\alpha = \alpha^L + \alpha^S$. Hence,

$$\alpha^S = \frac{\alpha}{1 + R}, \quad (8)$$

$$\alpha^L = \frac{R\alpha}{1 + R}. \quad (9)$$

For this investigation only three values of R were studied: $R = 1/3$, $R = 1$, and $R = 3$. To reach these values of R , the gas was injected through the small capillary bank until reaching the desired value of α^S ; then, the valve feeding the large capillary bank was gradually opened until the desired value of α was reached (by monitoring the increase in the column level).

A. Measurement of bubble velocity

In this study the bubble velocity, U_b , was determined with an image processing technique. As opposed to what has been used previously in our group [2,22], we opted for an image-based technique due to the difficulty involved in identifying velocity traces of two different bubble species with a single intrusive probe. To avoid having to implement a discrimination criteria, we determined the bubble velocity with a semimanual technique. The flow was filmed with a digital high-speed camera that was placed at midheight of the column. The images were processed with a Matlab code. A given bubble was identified manually in two consecutive frames (the bubble position was determined by locating three points of its edge). The program calculated the displacement of the bubble center in pixels; since the pixel/mm ratio and the image frame rate were known, the bubble velocity was calculated. A minimum of 300 bubbles were counted for each case to calculate both the mean and variance of the velocity. In this manner, it was possible to obtain accurate measurements of the mean bubble velocity for each size. However, the measurement of the variance were not statistically converged, so a large uncertainty was observed. Therefore, these measurements are not reported. Note that the present technique is limited to relatively dilute flows. If the same bubble cannot be identified in different frames, the measurement is not possible. Even if some bubble can be detected, the process becomes labor-intensive as many frames need to be checked to obtain the desired data sample.

B. Measurement of liquid velocity

To determine the liquid velocity, we used the flying hot-film technique developed by Martinez-Mercado *et al.* [2]. Here, we only describe the salient features of the technique. A hot-film probe is mounted on a holder, which displaces it at a known mean velocity. By subtracting the displacement velocity of the probe to the signal obtained, a true measure of the liquid velocity is obtained. This technique eliminates the shortcomings of the hot-film technique for small mean velocity measurements. As suggested by Martinez-Mercado *et al.* [2] and Mendez *et al.* [4], a displacement probe velocity of 10 cm/s was used. The system used was a IFA300 by TSI©, with a straight sensor (50 μm wire with a quartz coating). A sampling rate of 10 000 samples/s was used for all experiments. The measuring time for each experiment was about 4 s. To improve the statistics of the measurement, the measurement was repeated at least ten times for each flow condition.

The most important issue that needs to be addressed when using a hot-film probe in order to measure liquid velocities in a bubbly flow is the bubble detection. As it is well known, the interaction of the gas phase with the hot element of the probe causes a faulty signal that has been removed. We have used the method used by Mendez *et al.* [4] to deal with the bubble-probe interaction issue. We use an optical fiber detector, in the close vicinity of the hot film, to determine when a bubble is in contact with the probe. The signal during the interaction is then removed. The liquid velocity variance is calculated from the traces in between bubble contacts.

C. Single bubble measurements

To characterize the system, we conducted measurements of single bubbles rising in stagnant fluids. We used a cylindrical column of 40 cm in height and 8 cm in diameter. The cylindrical container was immersed in a rectangular vessel filled with the same liquid, to reduce optical distortion. The bubbles were injected through the bottom using the same two tube sizes used to build the capillary array. The three liquids listed on Table I were used. Nitrogen gas was pumped using a syringe pump considering a very small gas flow rate (about 1 $\mu\text{l/s}$) such that individual bubbles were produced at a small frequency. The motion was filmed with a high-speed camera. The results obtained for this

TABLE II. Experimental results for isolated bubbles. For each liquid, two bubble sizes were produced: large and small, L and S , respectively. The letters “o” and “s” correspond to the type of trajectory observed for each bubble, oscillating or straight, respectively. The Reynolds and Weber numbers are defined as $Re = \rho U_b d_{eq}/\mu$, $We = \rho U_b^2 d_{eq}/\sigma$, respectively. The superscript “0” refers to isolated bubble conditions.

Liquid (symbol)	d_{eq} mm	χ -	U_b^0 mm/s	Re^0 -	We^0 -	Trajectory -
S, water (●)	1.70	1.57	322.9	550	2.4	o
L, water (○)	3.68	1.93	278.7	1024	3.9	o
S, w-g 30% (◆)	1.96	1.52	272.7	229	2.3	s
L, w-g 30% (◇)	3.46	2.06	252.2	374	3.5	o
S, w-g 50% (■)	1.97	1.19	188.7	70	1.2	s
L, w-g 50% (□)	3.41	1.97	215.1	138	2.7	s

set of measurements are summarized in Table II. At least 10 measurements were conducted for each bubble size-fluid combination.

Figure 2 shows the measured velocities of isolated bubbles for the two capillary sizes used in this study. The size ratio obtained for the two bubble sizes, $\lambda \approx 1.9$, is approximately the same for the three liquids. Moreover, the comparison of the terminal velocity with that obtained from Moore’s prediction [23] shows that our experiment is relatively clean. Also, from this plot the key differences of the conditions tested in the bidisperse bubbly flow can be identified. For the case of water, the large bubbles rise at a slower rate than the smaller ones. This fact results from the deformation attained by air bubbles in water: since large bubbles are more oblate, their drag is in fact larger than that of smaller less deformed bubbles. In this case, the bubble velocity ratio is smaller than 1 ($\Gamma_1 = 0.86$). For this case, both small and large bubbles ascend following an oscillating trajectory. Now, on the other hand, when the 50-50 water-glycerin mixture is used, the larger bubbles ascended faster than the small ones because the bubbles are not very deformed. Hence, the bubble velocity

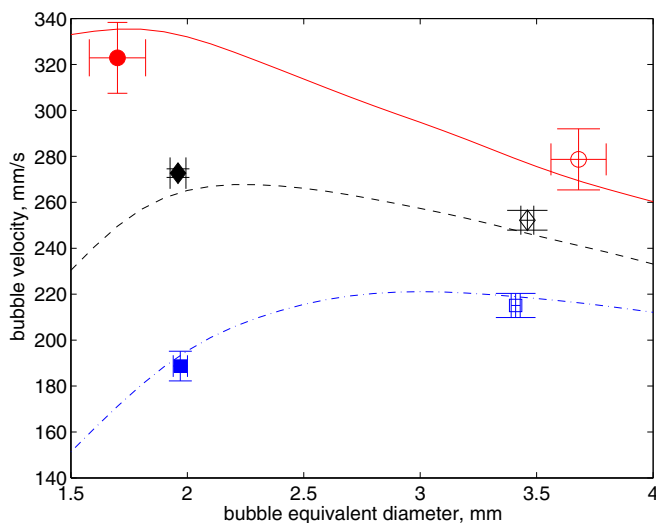


FIG. 2. Terminal bubble velocity as a function of equivalent diameter. The symbols denote experiments conducted in different liquids: (●,○), water; (◆,◇) water-glycerin 30%; (■,□) water-glycerin 50%. The filled and empty symbols refer to small and large bubbles, respectively. The lines show the predictions of Moore [23] for the three liquids used here: (—), $Mo = 2.6 \times 10^{-8}$; (---), $Mo = 3.9 \times 10^{-6}$; (- · - ·), $Mo = 3.1 \times 10^{-5}$.

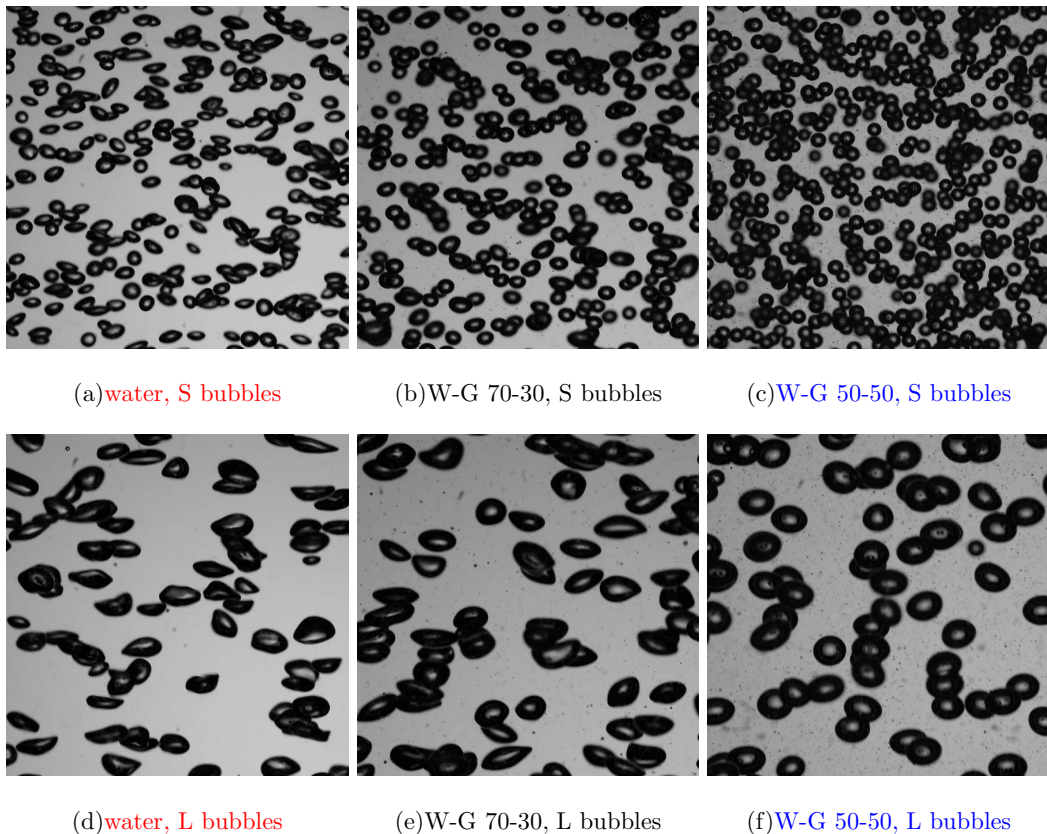


FIG. 3. Typical monodisperse bubbly flows. Images obtained for different liquids for a gas volume fraction of $\alpha = 0.02$. The top and bottom rows show images obtained for the small and large capillary array, respectively. Water, (a) and (d); water-glycerin (70-30), (b) and (e); water-glycerin (50-50), (c) and (f). The size of each image is approximately 5×5 , cm^2 .

ratio is greater than 1 ($\Gamma_1 = 1.14$). Also for this case, bubbles of both sizes ascend in a rectilinear fashion. For the intermediate case, the 70-30 water-glycerin liquid, the bubble velocity ratio is closer to unity ($\Gamma_1 = 0.93$); the large bubbles oscillate while the small ones follow a rectilinear trajectory. Therefore, with these combinations of bubble sizes and liquid viscosities we can explore the effects of varying Γ_1 and Γ_2 on the behavior of the bubbly flow.

III. RESULTS: MONODISPERSE FLOWS

First, we conducted a series of experiments for monodisperse flows to serve as a basis for comparison. Note that most of the results for monodisperse flows have already been published in Mendez *et al.* [4]; however, some information is reproduced here for clarity. Figure 3 shows images of monodisperse flows obtained with our setup. It is evident that the flows are nearly monodisperse. As the viscosity of the liquid increases, the shape of the bubbles becomes less deformed. For all flow conditions, the bubble diameter was observed to slightly increase with gas volume fraction. For instance, for water and the small capillaries, the bubble diameter for very dilute flows ($\alpha < 0.005$) grew from $d_b = 1.97$ mm to $d_b = 2.55$ mm when the gas volume reached a value of $\alpha = 0.06$ (about a 30% increase in size). The same amount of increase was observed for all cases.

The change of mean bubble velocity as a function as gas volume fraction for monodisperse flow can be found in Fig. 7 of Mendez *et al.* [4]. For all cases, the bubble velocity decreases with gas volume

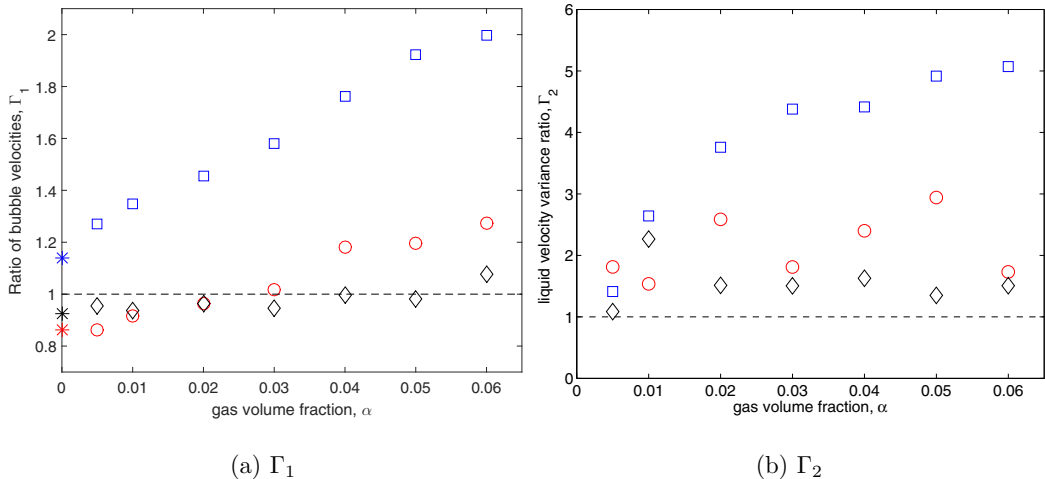


FIG. 4. Ratio of bubble velocities, $\Gamma_1 = U_b^L/U_b^S$, and ratio of liquid velocity variances, $\Gamma_2 = \langle U_l^2 \rangle^L / \langle U_l^2 \rangle^S$, as a function of gas volume fraction. All data is for monodisperse flows. The symbols denote experiments conducted in different liquids: (\circ), water; (\diamond) water-glycerin 30%; (\square) water-glycerin 50%. The asterisks (of each color) on (a) at $\alpha = 0$ represent the values corresponding to isolated bubbles, taken from Fig. 2.

fraction. The rate of decrease of the bubble velocity depends on the Reynolds and Weber number of the flow, as discussed by Mendez *et al.* [4]. There is not a simple direct correlation between the value of these dimensionless numbers and the bubble hinderance for each case. Figure 4(a) shows the bubble velocity ratio, Γ_1 , as a function of the gas volume fraction for the three liquids used here. This ratio considers the monodisperse data, with the aim to assess the relative effect of each bubble species. The behavior for each liquid is different. For water, Γ_1 gradually increases from a value smaller than one for small gas volume fractions to being close to 1.3 for the highest volume fraction. For the 70-30 water-glycerin mixture the ratio remains relatively constant around one for all gas volume fractions. For the fluid with the highest viscosity (50-50 water-glycerin), Γ_1 is always larger than unity and also gradually increases with gas volume fraction. These different scenarios are expected to affect the behavior of the bidisperse flow. It is interesting to determine if these ratios will remain unaffected if both bubble size species are present simultaneously.

The change of the liquid velocity variance with gas volume fraction for monodisperse flows, for each bubble size and liquid, was reported in Fig. 8 of Mendez *et al.* [4]. The liquid fluctuations, in all cases, increase with gas volume fraction; in normalized terms, considering the bubble terminal velocity in each case, the relative fluctuations are larger as the Reynolds number decreases. Figure 4(b) shows the ratio of liquid velocity variances, Γ_2 , as a function of gas volume fraction for monodisperse flow composed by either large or small bubbles. Clearly, for all three liquids, the variance induced by large bubbles is larger than that induced by small bubbles for all gas volume fractions. While for water and the 70-30 water-glycerin mixture ratio remains relatively constant for the range of gas volume fractions studied here, the 50-50 water-glycerin mixture shows that the ratio Γ_2 progressively increases with α . For the case of bidisperse flows, when the two bubble size species are present simultaneously, we can expect changes in both the mean bubble velocity and the liquid velocity fluctuations.

IV. RESULTS: BIDISPERSE FLOWS

Figure 5 shows typical images of bidisperse flows for the three liquids tested. For brevity, images are shown only for $\alpha = 0.02$. In particular, the images show how the bubble distribution changes with R . Again, according to the definition of R , a flow with $R < 1$ contains more volume of small bubbles than that of large bubbles. Respectively, $R > 1$ indicates the presence of more large bubbles

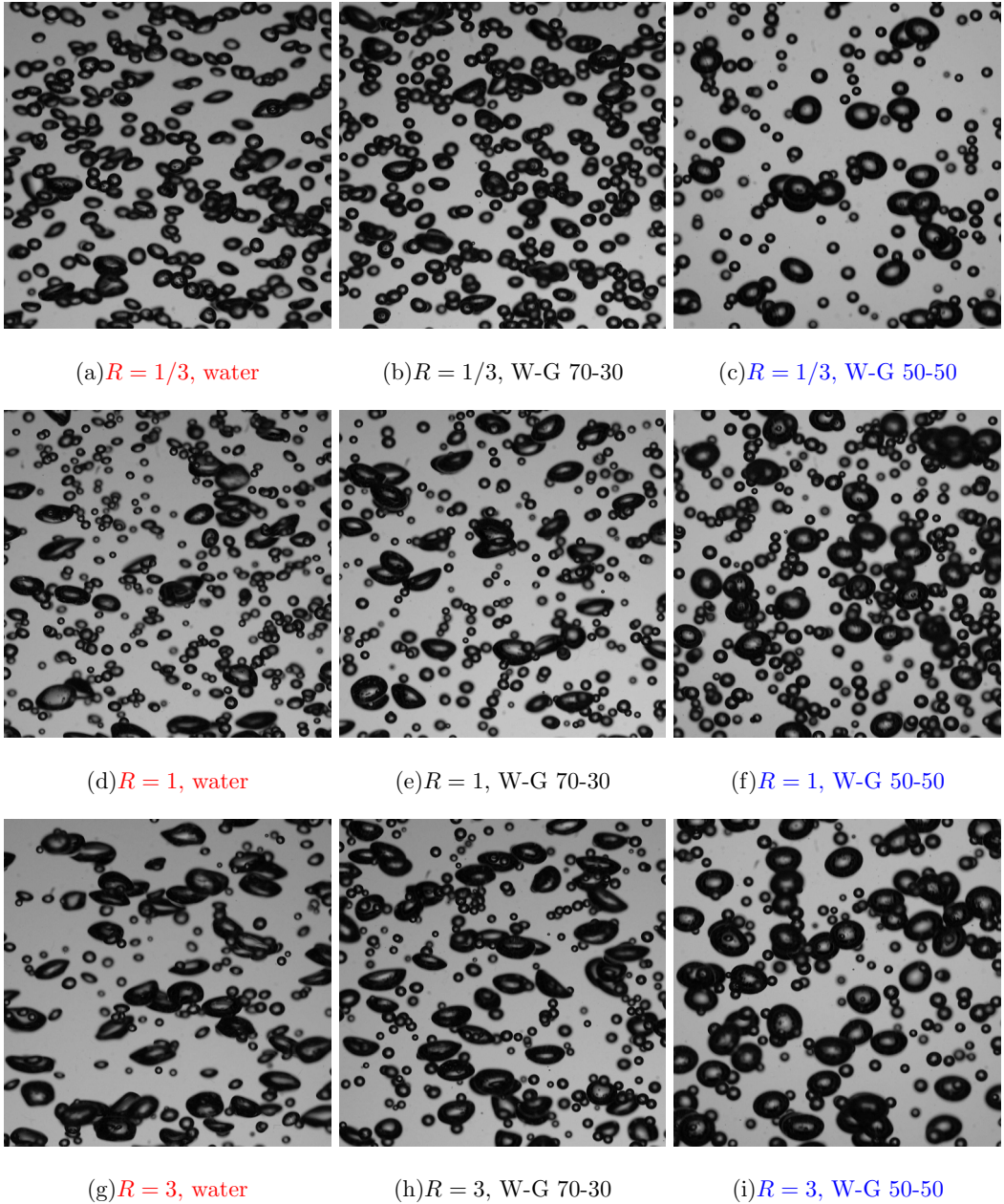


FIG. 5. Typical bidisperse bubbly flows. Images obtained for different liquids for a gas volume fraction of $\alpha = 0.02$. The top, middle and bottom rows show flows for the three values of the parameter R (1/3, 1 and 3), respectively. Water, (a), (d), and (g); water-glycerin (70-30), (b), (e), and (h); water-glycerin (50-50), (c), (f), and (i).

in comparison to small ones. The images in the figure are in clear accordance with the value of R . In all cases, the two bubble sizes are readily identified and no significant bubble clustering is observed. Similar distributions are observed for other gas volume fractions. Note that although the bubble size was fairly uniform when each capillary bank is operated independently (see Fig. 3), for the bidisperse experiments some size variation can be observed, especially for the small bubble size

species. Nevertheless, the images clearly show that a distinct bidisperse flow can be produced and controlled in each case.

A. Mean bubble velocity

Now, we can address the possible changes in the mean bubble velocity resulting from the fact that two size species are present. Note that, in principle, each size species moves at a different speed. Such a velocity difference could induce liquid velocity fluctuations and, as a result, change the character of the flow.

Figure 6 shows the bubble velocity as a function of gas volume fraction, for each species and each fluid for the three values of R . For comparison, the measurement obtained for the monodisperse case is shown in each case by the continuous or dashed lines. For the case of $R = 1/3$, Figs. 6(a) and 6(b), the mean bubble velocity for small bubbles does not change significantly with respect to the monodisperse case. This could be expected since this value of R indicates that small bubbles are more populous than larger ones. For water, the mean bubble velocity is within 5% of its monodisperse value and does not change with gas volume fraction. For the 70-30 water-glycerin liquid a reduction of the mean bubble velocity of about 10% is observed for all gas volume fractions. For the 50-50 water-glycerin liquid the small bubble velocity increases up to 30% from its monodisperse value, as the gas volume fraction increases up to 0.05. On the other hand, the mean bubble velocity for the large bubbles is smaller than that in the monodispersed case for the three liquids. This could be explained, again, from the fact that these large bubbles move in an environment dominated by small bubbles which could induce a change in the effective stress around them. For water and the 70-30 water-glycerin liquid, the large bubble velocity decreases about 20% (with respect to the monodisperse value) for the whole range of gas volume fractions. The reduction of velocity is about 10% for the 50-50 water-glycerin liquid for small gas volume fractions; for $\alpha > 0.05$, the mean bubble velocity is nearly the same as the monodisperse case. These trends for the large bubble species are in good qualitative agreement with the calculation of Kumaran and Koch [16].

The experiments corresponding to a value of $R = 1$ are shown in Figs. 6(c) and 6(d). In this case, the presence of large bubbles begins to affect the mean bubble velocity of the small bubble species more noticeably. For water, the bubble velocity of the small bubble species is reduced (90% of its monodisperse value) for small gas volume fractions but increased for larger volume fractions (up to 30% larger than the monodisperse value for $\alpha = 0.06$). For the 70-30 water-glycerin liquid, the bubble velocity is 10% smaller than its monodisperse value but preserves the same rate of change with gas volume fraction. For the 50-50 water-glycerin liquid, the behavior is similar to the $R = 1/3$ case: the bubble velocity increases with gas volume fraction from a value close to the monodisperse case to about 20% larger for $\alpha = 0.06$. For larger bubbles, the velocity is smaller than the monodisperse case for all volume fractions. For water and the 70-30 water-glycerin liquid the large bubble velocity is about 12% smaller than the monodisperse value and does not change with gas volume fraction. For the 50-50 water-glycerin liquid, the reduction of large bubble velocity is smaller, close to 5% and relatively constant with α .

The case for $R = 3$, for which gas volume fraction of the large bubble is larger, is shown in Figs. 6(e) and 6(f). This case behaves in a similar manner to the previous one ($R = 1$); more or less the same trends are observed in all cases and only some slight changes in the velocities for both species are identified. Note that although the gas volume fraction of large bubbles is larger, the number density of large bubbles is still smaller. The number density for each bubble species, the number of bubbles per unit volume, can be calculated as $n^i = 6\alpha^i / [\pi (d_{eq}^i)^3]$. Considering Eqs. (8) and (9), we can write

$$n^L = \frac{6}{\pi (d_{eq}^L)^3} \frac{R\alpha}{R+1}, \quad (10)$$

$$n^S = \frac{6}{\pi (d_{eq}^S)^3} \frac{1\alpha}{R+1}. \quad (11)$$

AVERAGE PROPERTIES OF BIDISPERSE BUBBLY FLOWS

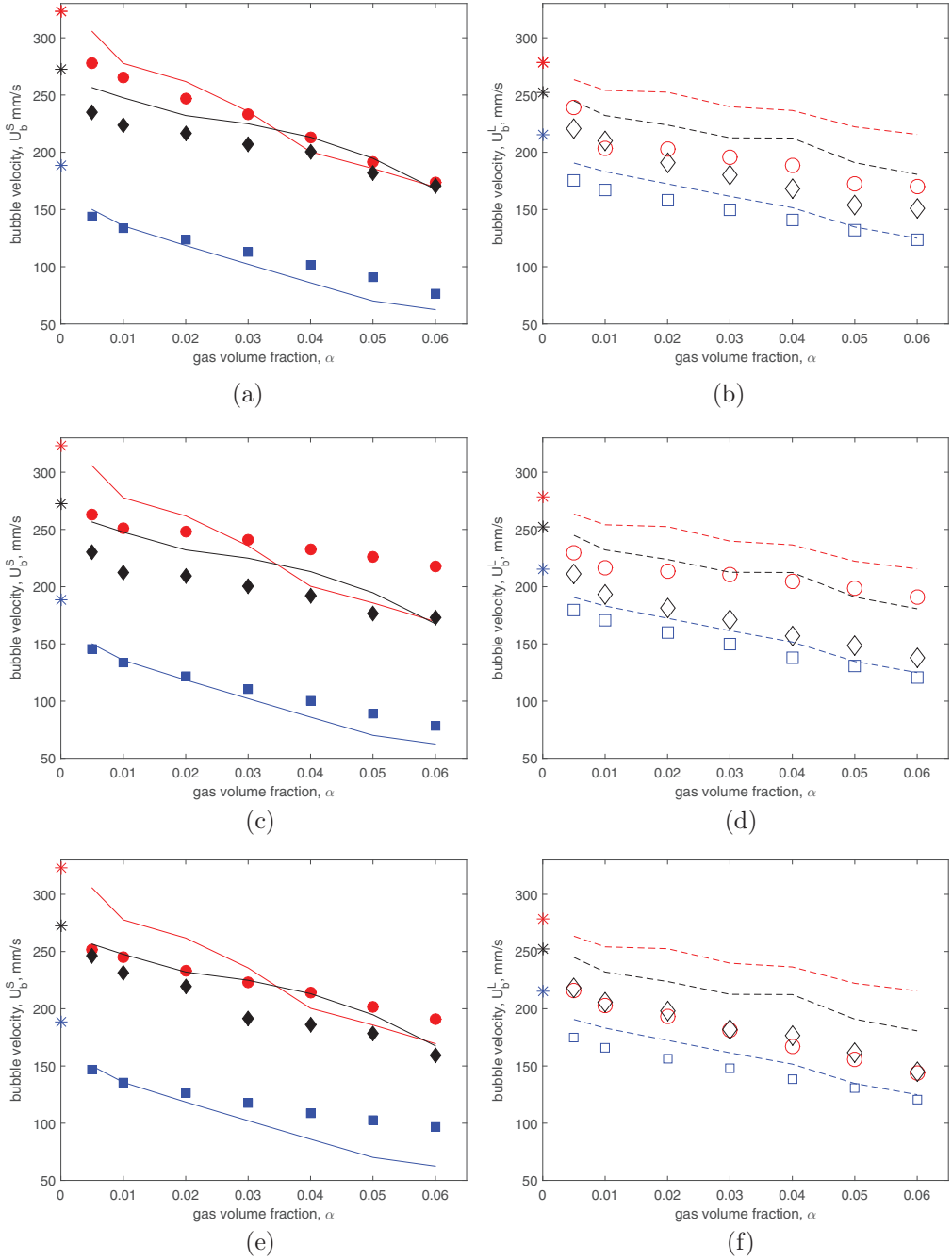


FIG. 6. Bubble velocity, U_b^i , as a function of gas volume fraction for bidisperse flows with i being S or L for small and large bubbles, respectively (left and right columns, respectively). The symbols denote experiments for different liquids: (\bullet, \circ) water; (\blacklozenge, \lozenge) water-glycerin 70-30%; (\blacksquare, \square) water-glycerin 50-50%. The filled and empty symbols refer to small and large bubbles, respectively. The continuous and dashed lines denote the bubble velocity for the monodisperse case for small and large bubbles, respectively. The asterisks (of each color) at $\alpha = 0$ represent the values corresponding to isolated bubbles, taken from Fig. 2. (a) S-bubbles, $R = 1/3$, (b) L-bubbles, $R = 1/3$, (c) S-bubbles, $R = 1$, (d) L-bubbles, $R = 1$, (e) S-bubbles, $R = 3$, and (f) L-bubbles, $R = 3$.

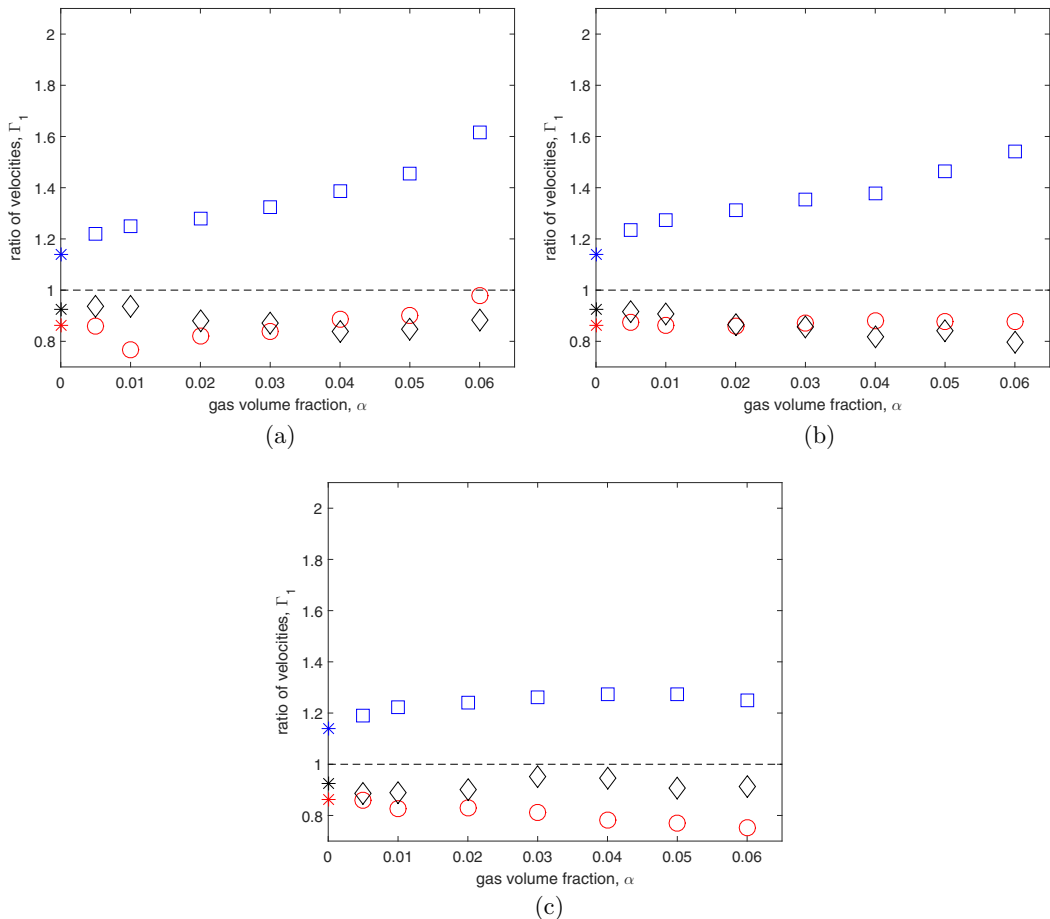


FIG. 7. Bubble velocity ratio, $\Gamma_1 = U_b^L/U_b^S$, as a function of gas volume fraction for bidisperse flows. The symbols denote experiments conducted in different liquids: (\circ), water; (\diamond) water-glycerin 70-30%; (\square) water-glycerin 50-50%. The asterisks (of each color) at $\alpha = 0$ represent the values corresponding to isolated bubbles, taken from Fig. 2. (a) $\Gamma_1, R = 1/3$, (b) $\Gamma_1, R = 1$, and (c) $\Gamma_1, R = 3$.

For instance, for the bubble sizes in Fig. 2, a value of $\alpha = 0.02$ (such as the images in Fig. 5), and $R = 3$, $n^L = 0.65$ bubbles/cm³ while $n^S = 1.19$ bubbles/cm³. In contrast, under the same conditions but for $R = 1/3$, $n^L = 0.22$ bubbles/cm³ and $n^S = 3.58$ bubbles/cm³. Therefore, to have 15 times as more large than small bubbles, the value of R would have to be 80. For the values of R used in this investigation, the small bubble species are always more populous than the large one. Hence, we can expect the small bubble species to be dominant.

Alternatively, the bubble velocity measurements for each species can be shown as a function of their proportional of gas volume fraction, α^S or α^L , considering Eqs. (8) and (9). In this manner, the bidisperse measurements for each species can be compared in a more direct manner with their corresponding monodisperse cases. In all cases the data is shift to the left (not shown), towards smaller values of α , depending on the value of R . The difference between the bidisperse and monodisperse measurements is larger and clearer.

The data in Fig. 6 can be presented in a different manner to quantify the amount of change of velocity as a result of the bidisperse nature of the flow. We consider the ratio Γ_1 , defined in Eq. (5), which is shown as a function of gas volume fraction, for all the bidisperse data, in Fig. 7. This ratio shows the relative magnitude of the velocity of each species for each R case, each liquid and for all

the gas volume fractions considered. For the three values of R , the same general trend is observed: for water and the 70-30 water-glycerin mixture, the small bubble velocity is larger than that of the big bubbles (within 20% difference and independent of α); for the 50-50 water-glycerin mixture, big bubbles have larger velocities than small bubbles for all gas volume fractions. The plots in Fig. 7 can be compared with that shown in Fig. 4(a), where the monodisperse data is shown. The behavior of Γ_1 shown in Fig. 4(a) would be expected in the bidisperse case if the two bubble size species did not interact with each other. Therefore, the differences between Figs. 4(a) and 7 can be attributed to the interaction between bubble species. For the monodisperse water case, Γ_1 went from being smaller to larger than one as the gas volume fraction increased. In the three bidisperse cases, the mean bubble velocity of the big bubble species is always smaller than the small bubble species. Again, for this liquid, the flow is dominated by the presence of small bubbles. For the 70-30 water-glycerin liquid, the behavior of the ratio Γ_1 of the bidisperse cases is close to that for the monodisperse case, being slightly smaller than 1 and constant with respect to α . In the case of the 50-50 water-glycerin liquid, the ratio Γ_1 is always larger than one: big bubbles always move faster than small ones. However, the value of Γ_1 becomes smaller as R increases. In the noninteraction case Γ_1 could be as large as 2; for $R = 3$, it barely reaches a value of 1.2 for $\alpha = 0.06$.

B. Liquid velocity variance

To quantify the amount of agitation in the liquid phase induced by the bubbles, we calculate the liquid velocity variance considering the measurement technique described in Sec. II B. In contrast to the bubble phase, the velocity fluctuations in the liquid phase are the result of the motion induced by the passage of large and small bubbles. In other words, the effect of each phase in the measurement of the liquid velocity cannot be separated for each one of the bubble size species.

Figure 8 shows the measured liquid velocity variance as a function of gas volume fraction for all the cases studied here: three liquids and three values of R . In all cases, the liquid velocity variance for the monodisperse flow is shown along with the bidisperse measurements. It is important to note that these measurements are more noisy than the bubble velocity measurements. Despite this fact, the trends are still clear. For all cases the velocity fluctuations increase with gas volume fraction, in accordance with what is observed in monodisperse flows. Regardless of the liquid and the value of R , the measured liquid fluctuations are higher than the monodispersed value for small bubbles for a given value of the gas fraction. For water and the 50-50 water-glycerin liquid, the measurements are smaller than the monodisperse value for large bubbles. In other words, for these two liquids the bidisperse measurements are in between the bounds of small and large bubbles. Interestingly, the liquid velocity fluctuations for the 70-30 water-glycerin liquid in the bidisperse flow can be larger than the monodisperse value for large bubbles. In this case, therefore, the bidisperse measurement can exceed the small or large bubble cases.

To assess the relative change of liquid velocity fluctuations resulting from the bidisperse nature of the flow, the following ratio can be calculated:

$$\Pi^i = \frac{\langle U_i^2 \rangle}{((U_i^2))_{\text{mono}}^i}, \quad (12)$$

where i is either S or L , corresponding to the monodisperse measurement for either small or large bubbles. Figure 9 shows the ratio Π^S (on the right) and Π^L (on the left) as a function of the gas volume fraction for the data shown in Fig. 8. There are several features that can be readily identified from the data, presented in this form. First, the liquid velocity fluctuations for the bidisperse flow are always larger than those measured for monodisperse flows with only small bubbles, Figs. 9(a), 9(c) and 9(e). In other words, the bidispersity induces more liquid velocity fluctuations in a flow, even if the number density of large bubbles, n^L , is small. Also, in this case, the ratio Π^S appears to increase with the value of R and to be relatively independent of α for the three liquids.

On the other hand, the value of Π^L , shown in Figs. 9(b), 9(d) and 9(f), is smaller than the monodisperse value for large bubbles for water and the 50-50 water-glycerin mixture. In other

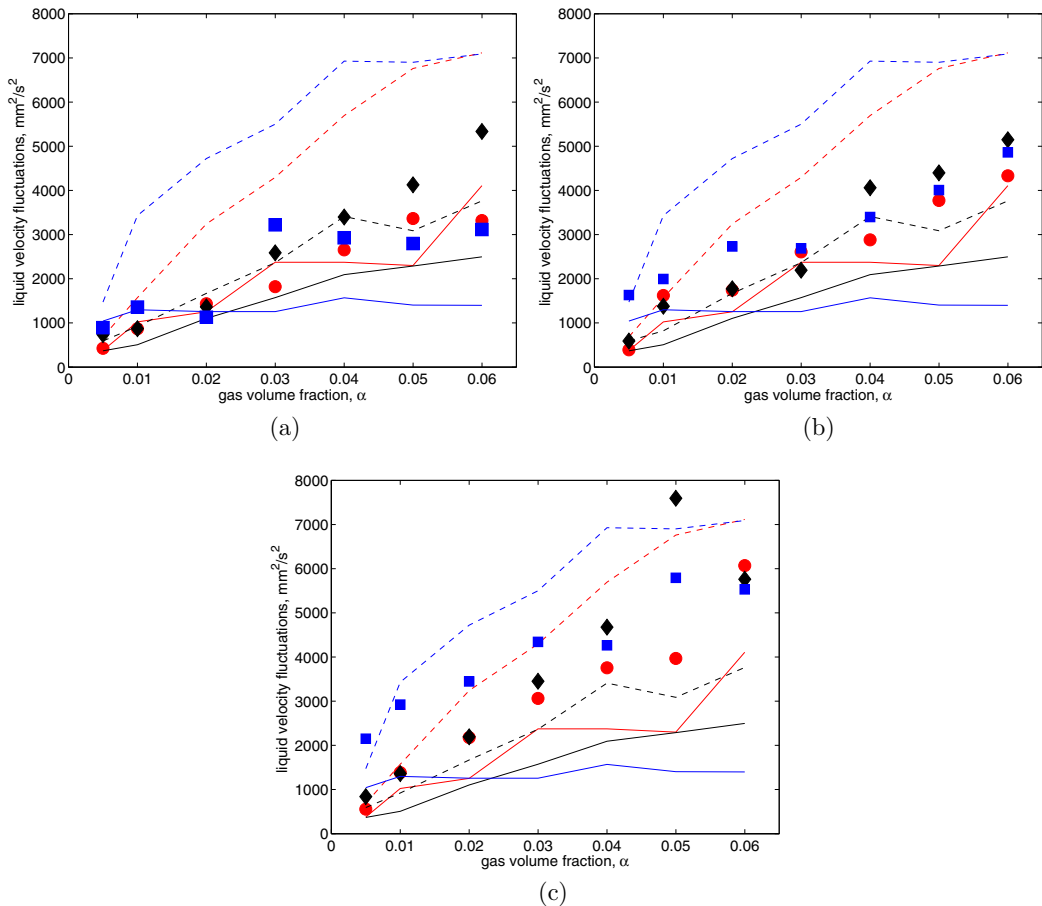


FIG. 8. Liquid velocity variance, $\langle U_l \rangle^2$, as a function of gas volume fraction for bidisperse flows. The symbols denote experiments conducted in different liquids: (●), water; (◆) water-glycerin 70-30%; (■) water-glycerin 50-50%. The continuous and dashed lines denote the liquid velocity variance for the monodisperse case for small and large bubbles, respectively. (a) $R = 1/3$, (b) $R = 1$, and (c) $R = 3$.

words, the agitation in the bidisperse media is always smaller than that of a monodisperse media composed only by large bubbles. Interestingly, for the 70-30 water-glycerin liquid, the ratio Π^L can be larger than 1: the liquid fluctuations can be larger than those for monodisperse flows with large bubbles.

1. Modeling the liquid velocity variance of a bidisperse flow

Considering the experimental results shown in Figs. 8 and 9, we can propose a simple expression to calculate the liquid velocity fluctuations for a bidisperse flow. The model is not intended to be predicted. Instead, it is used to determine whether or not the total fluctuation is simply the sum of that produce by each bubble species.

It is well known that for the case of bubbly flow with relatively large Re the liquid velocity fluctuations are

$$\langle U_l^2 \rangle = \kappa U_b^2 \alpha^n, \quad (13)$$

where κ is a constant of order 1 (which value depends on the bubble size) and $n \approx 0.4$ and $n \approx 0.8$ for small and large Re , respectively [2,24]. We can argue that, for a bidisperse bubble flow, each species

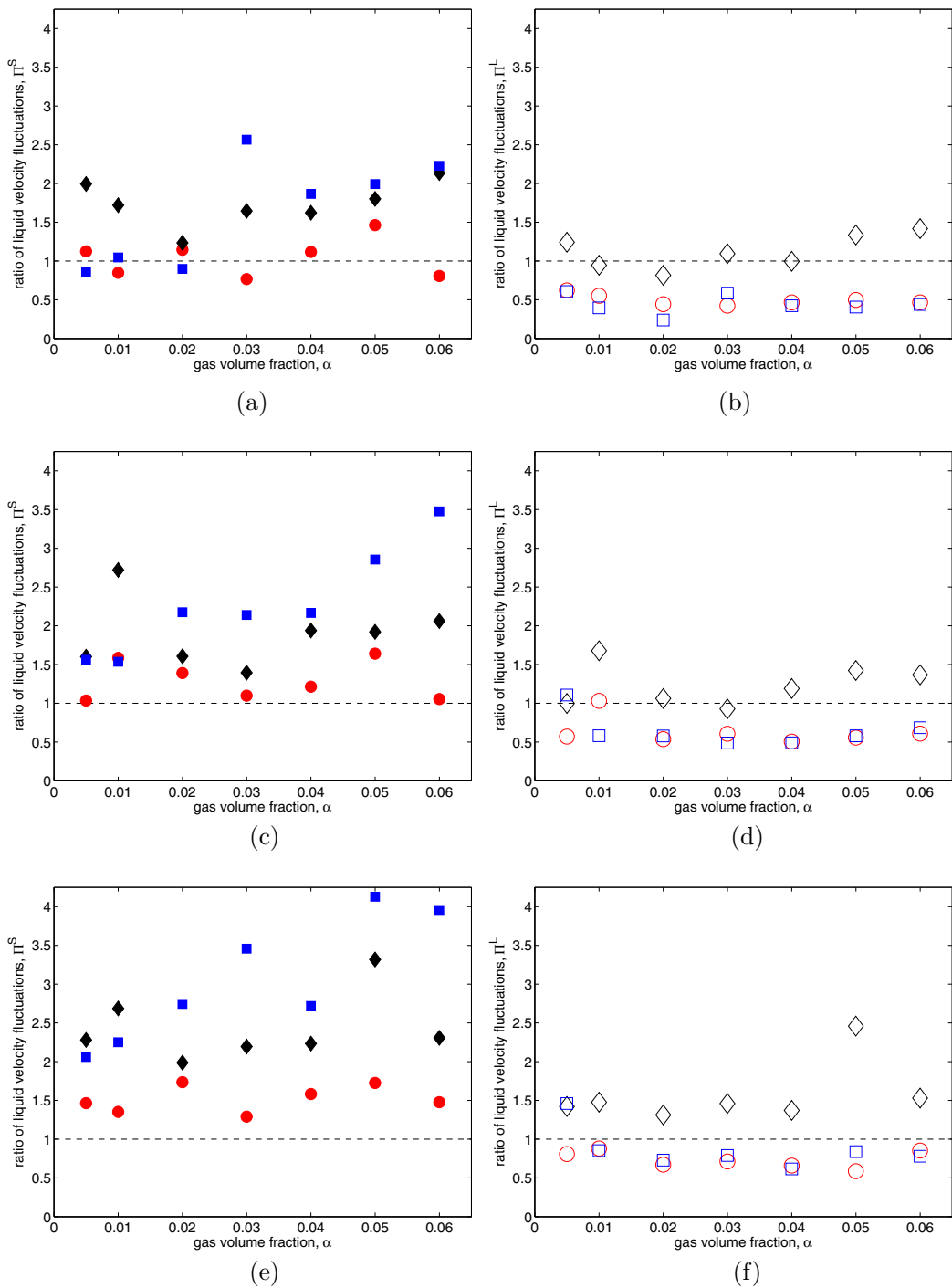


FIG. 9. Liquid velocity variance ratio, Π^S and Π^L (left and right columns, respectively), as a function of gas volume fraction for bidisperse flows. The symbols denote experiments for different liquids: (\bullet, \circ), water; (\blacklozenge, \diamond) water-glycerin 70-30%; (\blacksquare, \square) water-glycerin 50-50%. The filled and empty symbols refer to either Π^S or Π^L , respectively. (a) small bubbles, $R = 1/3$, (b) large bubbles, $R = 1/3$, (c) small bubbles, $R = 1$, (d) large bubbles, $R = 1$, (e) small bubbles, $R = 3$, and (f) large bubbles, $R = 3$.

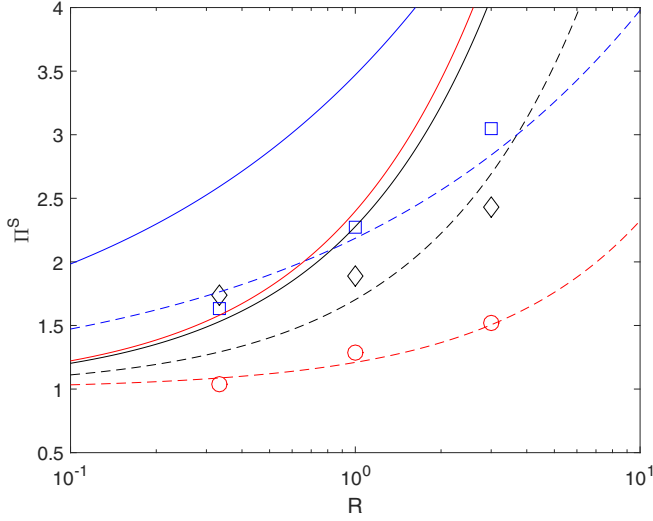


FIG. 10. Ratio of liquid velocity fluctuations, Π^S as a function of the gas volume fraction ratio, R , for the three liquids tested in this study: (○) water; (◇) water-glycerin 70-30%; (□) water-glycerin 50-50%. The lines show the predictions from Eq. (15). For water: $n = 0.8$, $\bar{\Gamma}_1 = 0.85$, $\kappa^* = 1.95$, $\kappa_{int}^* = -0.8$ (red lines); for water-glycerin 70-30%: $n = 0.8$, $\bar{\Gamma}_1 = 0.89$, $\kappa^* = 1.63$, $\kappa_{int}^* = -0.5$ (black lines); and for water-glycerin 50-50%: $n = 0.4$, $\bar{\Gamma}_1 = 1.32$, $\kappa^* = 1.41$, $\kappa_{int}^* = -0.52$ (blue lines). For all cases, the continuous lines represent the predictions considering $\kappa_{int}^* = 0$ (no interaction).

contributes individually to the generation of liquid velocity fluctuations. Furthermore, we can expect a dissipation (or enhancement) mechanisms to exist resulting from the interaction between species. Assuming that these contributions can be added linearly to the total liquid velocity fluctuations, and considering Eq. (13), we have

$$\langle U_l^2 \rangle = \kappa_S (U_b^2 \alpha^n)^S + \kappa_L (U_b^2 \alpha^n)^L + \kappa_{LS} [\kappa_L (U_b^2 \alpha^n)^L], \quad (14)$$

where κ_S and κ_L are proportionality constants for each species. The last term in the equation above represents the dissipation induced by the large bubble species on the total fluctuations, modeled through the coefficient κ_{LS} , which is negative (in this case).

Since the flows considered here are dominated by the presence of small bubbles, we can normalize Eq. (14) by $\langle U_l^2 \rangle^S$, to write

$$\Pi^S = 1 + \kappa^* (\Gamma_1)^2 R^n + \kappa_{int}^* [\kappa^* (\Gamma_1)^2 R^n], \quad (15)$$

where $\kappa^* = \kappa_L / \kappa_S$ and $\kappa_{int}^* = \kappa_{LS} / \kappa_S$. Clearly, Eq. (15) is only valid for the limit of small R .

From the data on Fig. 7, the value of Γ_1 can be determined for each liquid. We note that Γ_1 is relatively constant for most experiments (with the exception of the 70-30 water-glycerin liquid for $R = 1/3$ and $R = 1$). The value of κ^* can be determined from the experiments reported by Martinez-Mercado *et al.* [2] and Mendez *et al.* [4]. Therefore, since for our experiments R is known for each case, the experimental measurements can be compared with the prediction from Eq. (15) considering κ_{int}^* as a fitting parameter. Figure 10 shows the value of Π^S as a function of the ratio R for all the experiments conducted here.

For the three liquids Π^S increases with R : the agitation of the flow increases from the small-bubble value as the number of large bubbles increases. As the viscosity of the liquid increases, Π^S is larger (for a given value of R). In the plot, the predictions from Eq. (15) are shown considering two cases. First, the solid lines represent the case for which no dissipation mechanism is considered ($\kappa_{int}^* = 0$). Clearly, simply adding the liquid velocity fluctuations from each species (in proportion) leads to a

significant over prediction of total mean fluctuations for all liquids. This indicates that a dissipation mechanism must be included. Considering negative values of κ_{int}^* , the predictions are brought much closer to the experimental results.

The form in which the dissipation mechanism is included in Eq. (15) indicates that the fluctuations from the large bubble species are being partially dissipated. This can be rationalized by the fact that, in the flows considered here, there are many more small bubbles that surround the large bubbles. Such population distribution is mostly likely shortening the wake of large bubbles, leading to the dampening of the fluctuations produced by such large wakes. Also, the value of κ_{int}^* needed to match the experimental values is reduced as the Reynolds number decreases. Since the wake size is generally proportional to the Reynolds number [25], it is expected that this dampening effect would be more pronounced for large Re. Note, however, that the wake behind bubbles in a swarm has been shown to be attenuated with respect to the isolated bubble case [26]. Therefore, the issue cannot be resolved from these arguments. A more in depth analysis of the mechanism of dissipation of fluctuations is needed.

V. CONCLUSIONS

In this investigation we conducted experiments to measure the average properties of bidisperse bubbly flows. By designing a capillary bank with tubes with two different sizes and having independent gas inlets, bubbly flows with controlled gas volume fractions of each species were produced. In particular, measurements of the mean bubble velocity, for each size species, and the liquid velocity variance were obtained for gas volume fractions up to 6%, three different values of gas volume fraction ratio and three different liquids. For all cases, the small bubble species was more populous than the large one. We found that, for most of the tested conditions, the mean bubble velocity of the large bubble species is reduced (with respect to the monodisperse value). The mean value of the small bubble species can be increased, decreased, or remain unaffected depending on the conditions of the flow. The liquid velocity variance was found to be bounded by the monodisperse values of both bubble size species; for one particular set of conditions, the variance in the bidisperse flow could be larger than the monodisperse case. Such large value of liquid velocity fluctuations could be of practical interest. A model for the liquid velocity fluctuations that considers the superposition of the effect of each bubble species was proposed. The agreement between experiments and predictions was possible by considering that part of the fluctuations induced by the large bubble species are dissipated. The precise mechanism of dissipation remains unclear.

We did not observe concentration instabilities, which have been reported for other bidisperse flows [10,11]. However, we cannot ascertain that such heterogenous behavior does not happen in bidisperse bubbly flows. The range of volume fractions in which such behavior was observed in low Reynolds number sedimenting suspensions was higher than that studied here. It is possible that such species clustering could be observed in bubbly flows for gas volume fractions larger than 6%.

To continue with the understanding bidisperse bubbly flows and to, possibly, make use of their superior mixing characteristics, additional analysis tools are needed. In particular, the determination of probability density functions of bubble and liquid velocities are needed; the information in such distributions has been essential in the recent progress of understanding for monodisperse bubbly flows. Furthermore, the analysis of fluid velocity spectra can also be of significant value to understand the changes in the length and time scales that give rise to pseudoturbulent behavior. We plan to pursue such analysis of experimental results in future studies.

[1] N. Kantarci, F. Borak, and K. O. Ulgen, Bubble column reactors, *Proc. Biochem.* **40**, 2263 (2005).

[2] J. Martinez-Mercado, C. A. Palacios-Morales, and R. Zenit, Measurement of pseudo-turbulence intensity in mono-dispersed bubbly liquids for $10 < \text{Re} < 500$, *Phys. Fluids* **19**, 103302 (2007).

- [3] J. Martinez Mercado, V. Prakash, Y. Tagawa, C. Sun, and D. Lohse, On bubble clustering and energy spectra in pseudo-turbulence, *J. Fluid Mech.* **650**, 287 (2013).
- [4] S. Mendez, J. C. Serrano, and R. Zenit, Power spectral distributions of pseudo-turbulent bubbly flows, *Phys. Fluids* **25**, 043303 (2013).
- [5] F. Risso, Agitation, mixing, and transfers induced by bubbles, *Annu. Rev. Fluid Mechanics* **50**, 25 (2018).
- [6] G. K. Batchelor, Sedimentation in a dilute polydisperse system of interacting spheres. Part 1. General theory, *J. Fluid Mech.* **119**, 379 (1982).
- [7] G. K. Batchelor and C.-S. Wen, Sedimentation in a dilute polydisperse system of interacting spheres. Part 2. Numerical results, *J. Fluid Mech.* **124**, 495 (1982).
- [8] G. K. Batchelor, Sedimentation in a dilute dispersion of spheres, *J. Fluid Mech.* **52**, 245 (1972).
- [9] Y. Peysson and E. Guazzelli, Velocity fluctuations in a bidisperse sedimenting suspension, *Phys. Fluids* **11**, 1953 (1999).
- [10] R. H. Weiland, Y. P. Fessas, and B. V. Ramarao, On instabilities arising during sedimentation of two component mixtures of solids, *J. Fluid Mech.* **142**, 383 (1984).
- [11] G. K. Batchelor and R. W. Janse Van Rensburg, Structure formation in bidisperse sedimentation, *J. Fluid Mech.* **166**, 379 (1986).
- [12] V. Kumaran and D. L. Koch, Properties of a bidisperse particle-gas suspension. part 1. collision time small compared with viscous relaxation time, *J. Fluid Mech.* **247**, 623 (1993).
- [13] V. Kumaran and D. L. Koch, Properties of a bidisperse particle-gas suspension. part 2. viscous relaxation time small compared with collision time, *J. Fluid Mech.* **247**, 643 (1993).
- [14] P. Valiveti and D. L. Koch, The inhomogeneous structure of a bidisperse sedimenting gas-solid suspension, *Phys. Fluids* **11**, 3283 (1999).
- [15] M. Abbas, E. Climent, O. Simonin, and M. Maxey, Dynamics of bidisperse suspensions under stokes flows: Linear shear flow and sedimentation, *Phys. Fluids* **18**, 121504 (2006).
- [16] V. Kumaran and D. L. Koch, The effect of hydrodynamic interactions on the average properties of a bidisperse suspension of high Reynolds number, low weber number bubbles, *Phys. Fluids A* **5**, 1123 (1993).
- [17] M. F. Goz, B. Bunner, M. Sommerfeld, and G. Tryggvason, Direct numerical simulation of bidisperse bubble swarms, in *Proceedings of the Fourth International Conference on Multiphase Flow, May 27 – June 1, 2001, New Orleans, LA* (ICMF, 2001), pp. 1–11.
- [18] M. Goz and M. Sommerfeld, Analysis of bubble interactions in bidisperse bubble swarms by direct numerical simulations, in *Bubbly Flows, Analysis, Modelling and Calculation*, 1st ed., edited by M. Sommerfeld (Springer, Berlin, 2004), pp. 175–190.
- [19] J. Lu and G. Tryggvason, Effect of bubble size in turbulent bubbly downflow in a vertical channel, *Chem. Eng. Sci.* **62**, 3008 (2007).
- [20] I. Roghair, M. W. Baltussen, M. Van Sint Annaland, and J. A. M. Kuipers, Direct numerical simulations of the drag force of bi-disperse bubble swarms, *Chem. Eng. Sci.* **95**, 48 (2013).
- [21] C. Santarelli and J. Frohlich, Direct numerical simulations of spherical bubbles in vertical turbulent channel flow. influence of bubble size and bidispersity, *Int. J. Multiphase Flow* **81**, 27 (2016).
- [22] R. Zenit, D. L. Koch, and A. S. Sangani, Measurements of the average properties of a suspension of bubbles rising in a vertical channel, *J. Fluid Mech.* **429**, 307 (2000).
- [23] D. W. Moore, The velocity of rise of distorted gas bubbles in a liquid of small viscosity, *J. Fluid Mech.* **23**, 749 (1965).
- [24] A. Cartellier and N. Riviere, Bubble-induced agitation and microstructure in uniform bubbly flows at small to moderate particle Reynolds numbers, *Phys. Fluids* **13**, 2165 (2001).
- [25] R. Clift, J. R. Grace, and M. E. Weber, *Bubbles, Drops, and Particles* (Academic Press, San Diego, 1978).
- [26] F. Risso and K. Ellignsen, Velocity fluctuations in a homogeneous dilute dispersion of high-Reynolds-number rising bubbles, *J. Fluid Mech.* **453**, 395 (2002).